

# **RAPID DESIGN AND MANUFACTURE OF ULTRALIGHT CELLULAR MATERIALS**

W. Brooks\*, C. Sutcliffe, W. Cantwell, P. Fox, J. Todd, R. Mines.

Manufacturing Science and Engineering Research Centre

The University of Liverpool

\*w.brooks@liverpool.ac.uk

Reviewed, accepted August 3, 2005

## **Abstract**

This paper details the design, manufacture and testing of regular metallic lattice structures with unit cell sizes in the range 0.8mm to 5mm and truss elements of 100-500  $\mu\text{m}$  in diameter [1]. The structures were manufactured using Selective Laser Melting (SLM) technology from 316L stainless steel. Compression tests have shown yield loadings of over 3.5kN despite being only 18mm by 18mm by 10mm in height, the results are favourably comparable to current commercially available metallic foams. Software has been developed that creates slice files without the use of CAD software or STL files and is capable of producing lattices within a volume defined by a STL file.

## **Introduction**

### **1.1 Hierarchical structures**

Hierarchical structures are organised assemblages of units capable of conferring unique properties to a structure via optimisation over a large range of length scales. The architecture of cellulose aggregates in wood, or collagen aggregates in cartilage provide excellent examples of this. The ability to design and fabricate synthetic structures with similar characteristics would lead to components with remarkable properties for example outstanding strength and stiffness could be combined with excellent fracture toughness. Unfortunately the realisation of the potential of synthetic hierarchical structures has been limited, because the inability of current processing techniques to provide methods for the precise control of material variables over all levels of structural arrangement [2]. This work examines the production of regular open cell metallic structures (ROCMS), the first step in the production of optimised structural geometries.

### **1.2 Selective Laser Melting**

The method applied for the fabrication of the ROCMS in this work is SLM, a layer addition solid freeform fabrication technique. SLM uses powder which is melted by a laser, this molten material then solidifies to full density. The requirement for SLM metal components is a spherical particle shape powder in the range of 20-50 $\mu\text{m}$ .

The MCP Realizer SLM workstation uses a 100w CW Ytterbium fibre laser (IPG, Germany) operating within 1068-1095nm. The optical system consists of a dual axis galvanometer (Cambridge Technology, United Kingdom) and a 300mm or 150mm focal length lens (Sill, Germany) combining to produce a focused beam spot size of 80 or 30 $\mu\text{m}$  at 80 Watts. All processing occurs in an Argon atmosphere with no more than 0.2% O<sub>2</sub>.

The machine melts a line of powder by focusing on a point of the line, pausing for a pre-defined exposure time, moving a pre-defined point distance and repeating the process. The build is controlled using the propriety software Fusco. Process parameters varied in the experiments described in this paper are exposure time and laser power. The metal powder used was gas atomised, 316L stainless steel (Osprey Metal Powders, United Kingdom).

### 1.3 Computer Coding

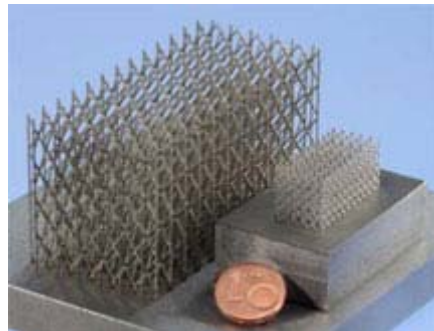


Figure 1: Original part file used for initial builds.

Successful samples created from the initial part file were sporadic. This file contained the slice data used produced the smaller structure shown in Figure 1. Inspection of the individual slices revealed poor scanning paths. Slices at regular intervals throughout the file had several points missing from layers and inappropriately placed scan lines. These errors caused missing strands, or over melted sections resulting in subsequent failure of the samples.

To correct these issues coding was developed to create a regular block of the lattice structure shown in Figure 1. This code created slice files directly layer by layer without slicing any CAD geometry. This gave the user the ability to define the extents of the part in the X, Y, and Z-axis, and the number of cells in each axis. To create this code the open source programming language Python [3] was used with wxPython [4] to create the user interface and the Visualisation Toolkit [5] to display and manipulate some of the data. These were downloaded in a compiled format from Enthought [6].

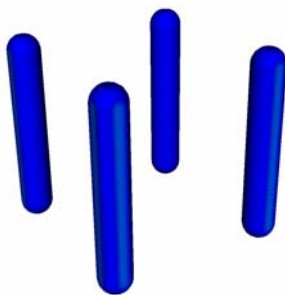


Figure 2: Pillar elements



Figure 3: Diagonal elements

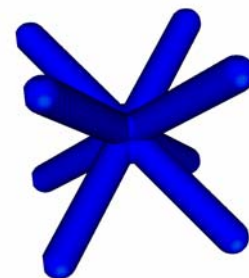


Figure 4: Octahedral elements

This code created a slice file for the lattice structure containing any combination of three lattice element types; pillar shown in figure 2, diagonal shown in figure 3, and octahedral elements shown in figure 4.

The corners for each cell give the co-ordinates for the scan vectors which create the pillar elements. The scan vectors for the diagonal elements are found using the proportion of the Z-height through the cell. This process is repeated throughout the layer with the co-ordinates output to a text file.

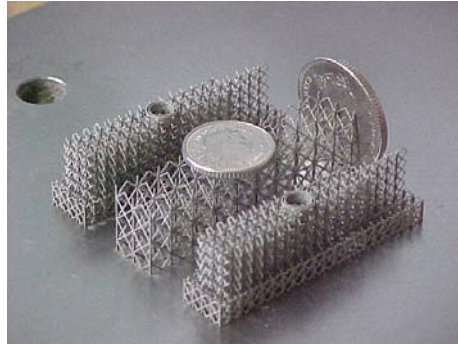


Figure 5: CAD bound lattice structures

Figure 5 shows the results of further development of this simple code to enabling the regular lattices to be clipped to an STL file.

## Experimentation

### 2.1 Compression Testing



Figure 6: Cell Type A

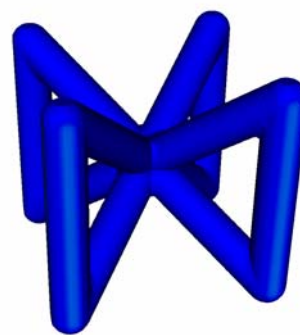


Figure 7: Cell Type B

Figure 6 and 7 show the two standard geometries used in the initial mechanical investigation to evaluate the changes in performance of Regular Open Cell Metallic Structures (ROCMS) when the laser exposure settings were changed. Figure 6 shows Cell Type A, a pillar and diagonal repeating cell and figure 7 shows Cell Type B a pillar and octahedral repeating cell.

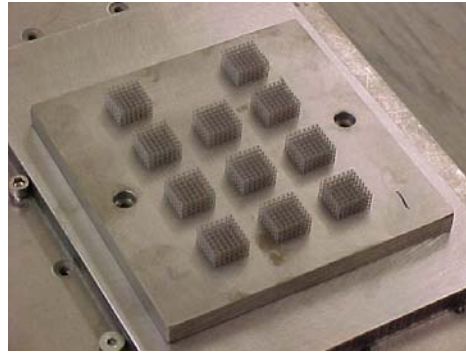


Figure 8 Compression test layout

A number of uni-axial compression tests were carried out to assess the effect that changing the laser exposure time had on the yield strength of the structures. Figure 8 shows an early build laid out in such a way that the structures could be tested without being removed from the substrate. This avoided adding additional error which could have been caused by damage to the structures when removed from the substrate.

Compression tests were carried out on a tensile testing machine (Instron 4505) equipped with a 10kN load cell. The cross head speed was set at a constant of 3mm/min for all of the tests. The samples were prepared by removal of the loose powder and greasing of the contact face of the samples. In addition to the uni-axial compression tests each sample was weighed using a 4d.p. mechanical balance to enable the yield crush data to be reported as specific strength.

## 2.2 Low Angle Elements

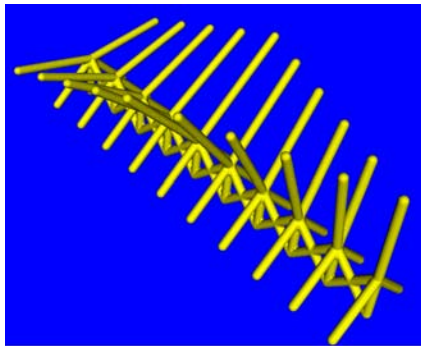


Figure 9 Computer image of test sample

```
POINTS 8 float
0 0 0
1 0 0
1 1 0
0 1 0
0 0 1
1 0 1
1 1 1
0 1 1
LINES 4
0 4
1 5
2 6
3 7
```

Figure 10 Text custom lattice input file describing four vertical pillars

Figure 9 shows a custom built lattice structure using the most recent version of the software. A text input file was created which listed all the co-ordinates of the ends of the elements and a second list of double IDs which referred to the original list of co-ordinates. Figure 10 shows a simplified version of the file format used describing four vertical pillars.

The custom lattice shown in figure 9 was used to test the minimum angle of element from the horizontal that could be created over a range of processing parameters.

## Results & Discussion

### 3.1 Variance of Compression Test Results

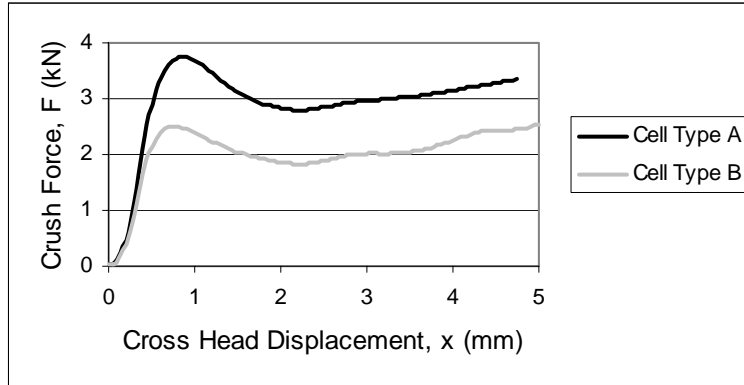


Figure 13 Crush profile of the two cell geometrys with 4000 $\mu$ s exposure

Figure 13 shows the difference in strength of the two lattice cell types. These plots are 100 data points per line with each line being an average from nine samples taken from one build as shown in figure 8.

Each individual sample used the same processing parameters for each scan vector in the slice file. Comparisons between the lower angle and vertical angle elements revealed that with identical processing parameters the element diameter reduces with the element angle. This was particularly apparent for Cell Type B which has lower angle elements than Cell Type A

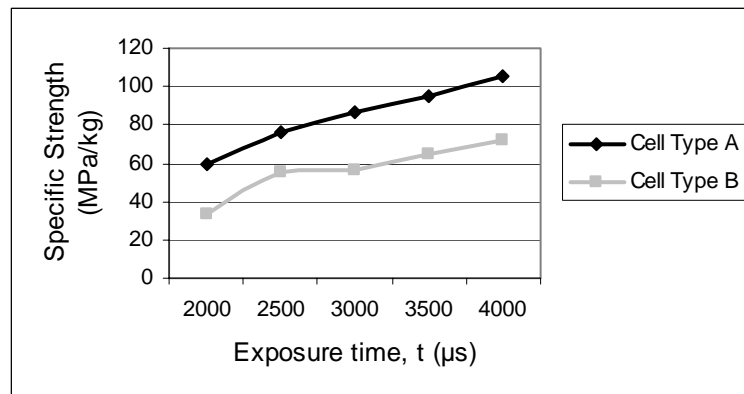


Figure 14 Yield strength of the two cell geometries with various exposures

Figure 14 shows the yield strength of both cell types plotted against the exposure setting that the sample set was built at. Each value is an average first peak value from nine samples of the same build.

From figure 14 it can be seen that the strength of the structures within this range of exposure settings rises in a linear fashion with the yield strength of Cell Type A remaining a constant amount above Cell Type B.

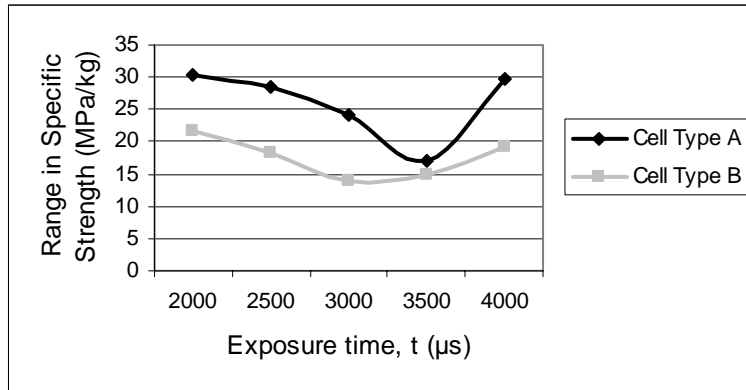


Figure 15 Range in specific strength versus exposure time

Figure 15 shows the range in specific strength within one exposure set of nine samples. It is clear that the 3500 exposure setting for the cell type A structure and 3000 for B offered the least range in specific strength. This demonstrates the ability to minimise process variance by adjusting process parameters. This would benefit these structure when used in engineering applications as it will enable the use of smaller safety factors, thus reducing the weight of the final product further.

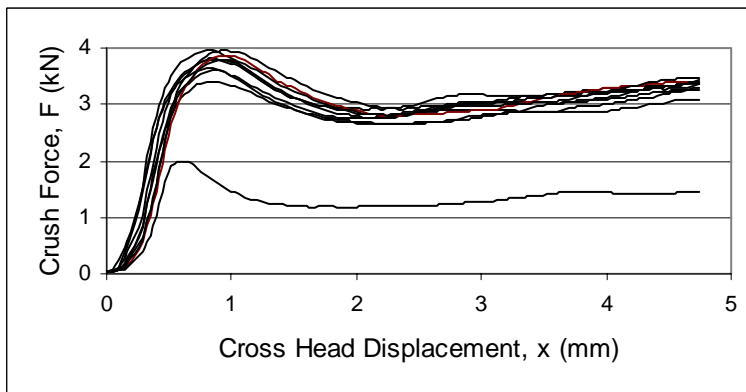


Figure 16 All crush profiles of one build of Cell Type A with 4000 $\mu\text{s}$  exposure

Figure 16 demonstrates the repeatability of the results these structures from one build. The lower line is not built at the same exposure setting as the rest. This line is the crush profile of the control sample which remained the same throughout the five builds of the cell type.

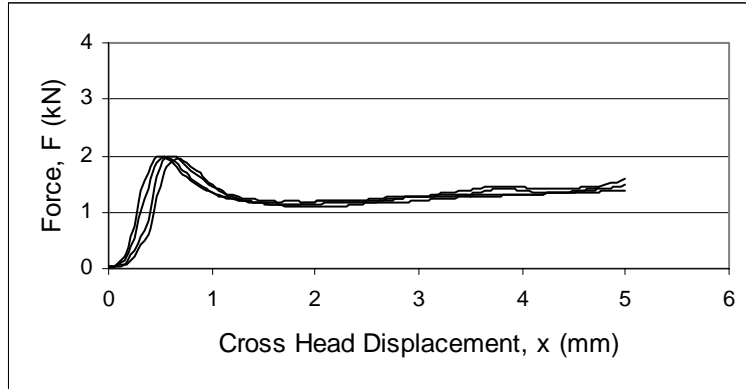


Figure 17 All control samples from five builds of Cell Type A

The purpose of the control sample was to check for variations in yield strength due to results being taken from different builds. When Figure 17 is compared to Figure 16 it is clear that there is greater variation due to position in the build than that caused by parts being build on different builds. This was investigated further.

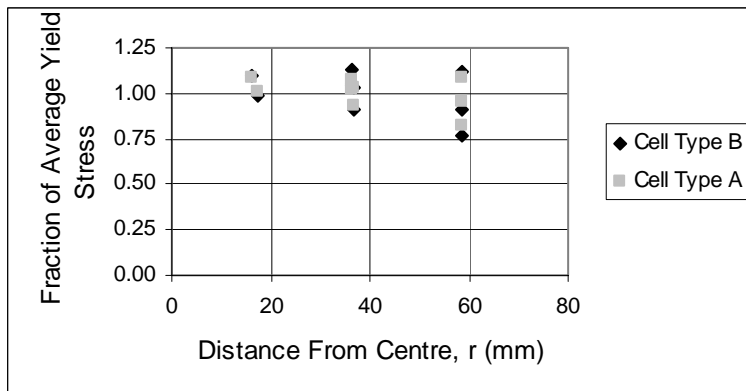


Figure 18 Yield stress as fraction of builds average yield stress compared to distance from centre.

For each build an average yield stress was calculated from measured data and the yield stress from each sample within this build was compared to this average. This was repeated for each build in each cell type with the results for each location being averaged (five samples per average) and the results plotted against the distance from the centre of the build. The results are shown in Figure 18.

This figure shows that there was a downward trend in strength as the placement of the samples moved further from the centre. There is also an unexpectedly close correlation in this characteristic across cell types. This indicated that the positional strength characteristic is independent of cell type suggesting that there is a machine specific variation occurring.

### 3.2 Lowest Low Angle Links

Laser Power (mA Pump Current)	Laser Exposure, t ( $\mu$ s)		
	2500	3000	3500
1500	1	3	6
2000	2	4	7
2500	Trial set	5	8

Table 1 Laser power and exposure for each group

Both builds of the low angle links contained an array of twenty-five samples. The first build - the trial set - was created using a safe laser power and exposure setting that had been used to create lattices with success before. The second build contained eight sample sets each built with different processing parameters, none of which were the same as the original trial set. Sample sets one to seven in the second build contained three samples, the eighth had four. To avoid problems with the position of build as much as possible the samples were randomly allocated a position on the build close to the centre.

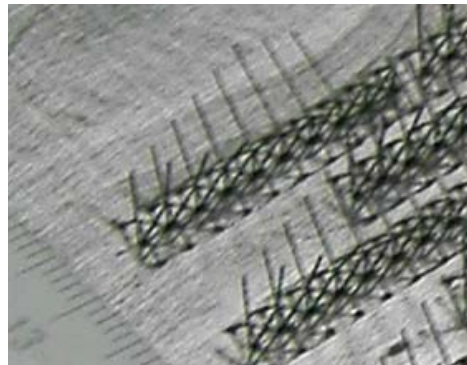


Figure 20 Low angle link test parts with millimetre scale

A scoring system was devised to rank the success of each of the samples. A score of one was allocated for a completely built element, zero for any less. Each angle was built twice on each part apart from the vertical pillar which was built once, as can be seen in figures 20 and 9. The success of the part was the sum of the scores divided by the total number of links.



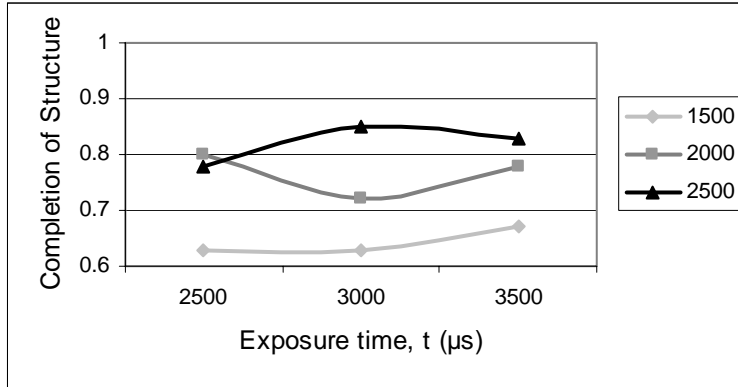


Figure 21 Success of links against exposure

Within the range of laser power and exposure covered in this test it can be seen that the effect of raising the laser power has a greater effect on the success of the structure than raising exposure time. This is illustrated by the level gradient of figure 21 and the upward gradient of figure 22.

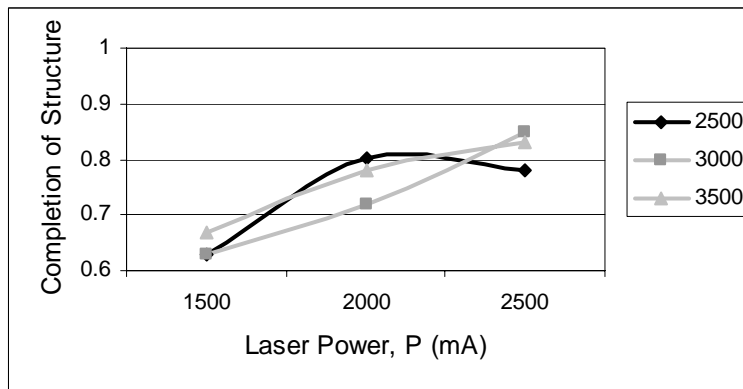


Figure 22 Success of links against laser power

With sample set eight of the low angle links building at least one of the two links in all four samples down to thirty-one degrees, as shown in table 2.

Sample	Angle										
	90.00	78.69	63.43	59.04	51.34	45.00	38.66	30.96	21.80	11.31	Aver
1	1	1	1	1	1	1	1	1	0	0	0.80
2	1	1	1	1	1	1	1	1	0.50	0.50	0.90
3	1	1	1	1	1	1	1	0.50	0	0	0.75
4	1	1	1	1	1	1	1	0.50	1	0	0.85
Aver	1	1	1	1	1	1	1	0.75	0.38	0.13	0.83

Table 2 Results of the low angle link test sample set eight.

## **Conclusions**

### **4.1 Exposing Weakness in Order to Improve**

The lattice compression test samples were selected for reliable build with the first set of mechanical testing. These showed the variation but the low angle link sample, which was designed to find the processing envelope, had features which were known in the design stage to not build reliably, features that would defiantly build, and a range of other features between. This highlighted the variation across a build and gave a test that can give results with just a visual inspection rather than lengthy compression tests. This is ideal for a run of builds over a short timeframe to cover the maximum number causes for the variation and reduce it.

It is apparent that location on the build area effects part quality. Parts built in a certain location on a build are being built at a constant quality indicating that the main cause for large range of yield stresses of the compression test samples is not due to a random variation which indicates that further study may be able to isolate and reduce the cause of the large range in results. This range has only been reported when building the lattice structures and has not been noticed when building solid parts. Pushing the machine to create parts at the limits of its capability has given a tool to isolate and improve the cause for range of quality of parts.

### **4.3 Success of Low Angle Elements**

The angles that can be built were much lower than expected. The highest exposure and laser power tested – sample set eight – successfully built all links down to thirty-eight degrees and had one success as low as eleven degrees.

It was unexpected to get any successful links with a build angle of eleven degrees. The laser spot size of the machine is forty microns and the spacing between points on subsequent layers is quarter of a millimetre, over six times the spot size.

## **Further Work**

### **5.1 Low Angle Links**

It is believed that increasing the length of the scan vectors used to build the low angle links and controlling them with separate processing parameters will greatly increase the success of the low angle links. Reliable horizontal links created on a single slice is the ultimate aim.

### **5.2 Link Testing**

As observed with both the compression test builds and the low angle links build quality of the links is affected as the link angle is reduced. For a full study of these structures this needs to be investigated, the simplest method for which will be the tensile testing of links build at particular angles, scanning techniques, and parameters.

This will be essential to gain a better understanding of the process and should be complimented by optical and metallurgical analysis. This all will be beneficial when modelling these structures for study into lattices that are conformal to volumes, or optimised for stress distribution, weight, or stiffness in the future.

### **5.3 Machine Deveolpment**

As part of the study into these structures it is essential that the end goal is not lost, the application of these structures in industry. To make this more viable constant effort should be made to continually reduce variance, increase build speed, and success of the parts.

The low angle link test build has shown itself to be a very quick method to evaluate what affect changes to the machine have on the success and range in quality of parts built. This method will be developed and tested with an initial aim to level out the variations in part quality within the build area so that the part quality no longer follows patterns dependant on its position.

#### **References**

- [1] Brooks WK, Todd J, Sutcliffe CJ; The Production of Open Cellular Lattice Structures Using Selective Laser Melting, 6<sup>th</sup> National Conference on Rapid Prototyping, Design, and Manufacturing 2005.
- [2] Hierarchical Structures in Biology as a Guide for New Materials Technology: NMAB, 464, National Research Council, Natl Res Council.
- [3] Python, [www.python.org](http://www.python.org).
- [4] wxWidgets, [www.wxwindows.org](http://www.wxwindows.org).
- [5] Kitware, [www.kitware.com](http://www.kitware.com)
- [6] Enthought, [www.enthought.com](http://www.enthought.com)